Published in final edited form as:
Exp Cell Res. 2013 March 10; 319(5): 623–632. doi:10.1016/j.yexcr.2012.12.028.

IFT80 is essential for chondrocyte differentiation by regulating hedgehog and Wnt signaling pathways

Changdong Wang[a], **Xue Yuan**[a], and **Shuying Yang**[a,b,*]

[a]Department of Oral Biology, School of Dental Medicine, State University of New York at Buffalo, Buffalo, NY 14214, USA

[b]New York State Center of Excellence in Bioinformatics & Life Science, Buffalo, NY 14263, USA

Abstract

Partial mutation of intraflagellar transport 80 (IFT80) in humans causes Jeune asphyxiating thoracic dystrophy (JATD) and short-rib polydactyly (SRP) syndrome type III. These diseases are autosomal recessive chondrodysplasias that share clinical similarities, including shortened long bones and constricted thoracic cage. However, the role and mechanism of IFT80 in the regulation of chondrocyte differentiation and function remain largely unknown. We hypothesize that IFT80 is required for the formation and function of cilia and plays a critical role in chondrogenic differentiation by regulating Hedgehog (Hh) and Wingless (Wnt) signaling pathways. To test this hypothesis, we first analyzed the IFT80 expression pattern and found that IFT80 was predominantly expressed in growth plate chondrocytes and during chondrogenic differentiation. Silencing IFT80 impaired cilia formation and chondrogenic differentiation in mouse bone marrow derived stromal cells (BMSCs), and decreased the expression of chondrocyte marker genes—collagen II and aggrecan. Additionally, silencing IFT80 down-regulated Hh signaling activity whereas up-regulated Wnt signaling activity. The overexpression of Gli2 in IFT80-silenced cells promoted chondrogenesis and recovered the chondrogenic deficiency from IFT80 silencing. Overall, our results demonstrate that IFT80 is essential for chondrocyte differentiation by regulating the Hh and Wnt signaling pathways.

Keywords

Intraflagellar transport; Cilia; Chondrogenic differentiation; Hedgehog signaling; Wnt signaling

Introduction

Cilia are highly conserved microtubule-based organelles that project from the cell surface into the extracellular environment and play essential roles in vertebrate development, signaling, cellular motility, sensory transduction, and homeostasis [1,2]. There are both motile cilia (9+2 microtubular pattern) and nonmotile, or primary cilia (9+0 microtubular pattern) [3,4]. Construction of the axoneme of cilia requires effective intraflagellar transport (IFT), a bidirectional transport system run by IFT protein complexes. The role of IFT in the assembly and maintenance of cilia has been intensively studied [2,5]. Accumulating evidence has demonstrated that defects in some IFT proteins, such as IFT88 [6] and IFT172 [7] results in impaired cilia formation, which contributes to ciliopathies in mouse models

*Corresponding author at: Department of Oral Biology, School of Dental Medicine, State university of New York at Buffalo, B36 Foster Hall, 3435 Main St, Buffalo 14214, NY 14214, USA. Fax: +1 716 829 3942. sy47@buffalo.edu (S. Yang).

[8,9] and/or humans [10]. Interestingly, defective other IFT proteins such as IFT25 and IFT27 do not affect cilia formation, but cause severe developmental and functional abnormalities in mouse models [11–13]. These results indicate that different IFT proteins probably have their distinct functions in cell process. So far, it remains largely unknown how IFT proteins contribute to chondrocyte differentiation and function during bone development and remodeling.

Primary cilia are present on almost every vertebrate cell, and their existence on chondrocytes was first reported about 40 years ago [14,15]. Later Poole and Jensen groups further analyzed the ultra-structure and function of primary cilia in chondrocytes [16,17]. Their and other studies suggested that primary cilia might serve as mechanical or chemical sensors in chondrocytes to mediate normal cell-extracellular matrix communication, which is required to maintain normal cellular orientation, growth and differentiation [18–21]. Additionally, osteoarthritis (OA) [22] is a disease associated with chondrocyte differentiation and function. Some studies demonstrated that primary cilia are present in normal cartilage as well as in mild and severe OA tissues [23]. Compared to normal cartilage, the proportion and length of the cilia in OA tissues are increased with OA severity at the eroding articulating surface [23]. Inflammatory cytokines such as interluekin-1 (IL-1), which are highly expressed in OA, are able to induce the elongation of the cilia [24]. Cultured chondrocytes from the patients with SRP syndrome showed morphologically abnormal, shortened cilia and abnormal cytoskeletal microtubule architecture [25]. In mouse models, deletion of IFT88 or Kif3a during chondrocyte development using the Col2α1-Cre promoter, causes a progressive loss of the cartilaginous growth plate and postnatal dwarfism that resembles the phenotype of mice with a conditional deletion of India Hedgehog (Ihh) induced in postnatal cartilage [26–28]. IFT88 deletion also results in symptoms of early OA due to reduced Hedgehog (Hh) signal repression by Gli3 [29]. Collectively, these findings highlight that IFT/cilia proteins play critical role in the differentiation and function of chondrocytes and chondrocyte-related diseases.

Much evidence revealed that there are connections between the Hh signal pathway and the primary cilium as well as IFT [9,30,31]. For example, conditional deletion of Kif3a causes abnormal Hh signaling topography, growth plate dysfunction, and excessive bone and cartilage formation during mouse skeletogenesis [32], which is similiar to the phenotype in Ihh-deficient mouse [33]. Gli transcription factors (Gli1, Gli2 and Gli3) are key effectors of the Hh signaling pathway [34]. Recent studies demonstrated that Gli transcription factors as well as several other Hh pathway components, including Smoothen (Smo) and Hh receptor Patched (Ptch), are accumulated in primary cilia either under resting conditions or during pathway activation [35]. Gli1 is dispensable for embryonic development and encodes a secondary mediator of Hh signaling [36]. Gli2 are the major transcriptional activator whereas Gli3 is the repressor of the mammalian Hh pathway [34,37]. These findings suggest the relationship between IFT/cilia and Hh/Gli and their roles in chondrocyte differentiation and function. In addition, Wnt signaling has been implicated in a wide variety of developmental processes from cell proliferation to cell fate determination and differentiation [38,39]. Wnt/β-catenin signals developmentally regulate chondrocyte differentiation, growth plate assembly and cartilage integrity [40]. Mice with transient activation of Wnt/α-catenin induced premature closure of the growth plate in postnatal mice [41]. Loss of primary cilia has been shown an increase in response to the canonical Wnt signaling pathway [42,43], suggesting that primary cilia/IFT proteins, at least some of them have a role in restraining Wnt/α-catenin signaling.

IFT80 protein is a recently-defined component of IFT complex B [44]. Loss of IFT80 in zebrafish results in cystic kidneys and a reduced number of cilia, whereas silencing IFT80 in *Tetrahymena thermophila* produces shortened or absent cilia [44,45]. Furthermore, IFT80

mutations in humans cause JATD [44] and SRP syndrome type III [46]. Those phenotypes suggest that mutation of IFT80 possibly affects chondrocyte differentiation and function. However, the precise role and mechanism of IFT80 in regulating chondrogenic differentiation remain unknown. Hence, in this study, our aim is to elucidate the role of IFT80 in cilia formation and chondrocyte differentiation and to identify the pathways involved in this progress. We first tested the expression pattern of IFT80 in growth plate and during chondrocyte differentiation. Furthermore, we used lentivirus-mediated small hairpin RNA (shRNA) to silence IFT80 in mouse BMSCs and characterized the effect of IFT80 silencing in cilia formation and chondrocyte differentiation in vitro. Additionally, we analyzed the mechanism by which IFT80 regulates Hh signaling and Wnt signaling pathways. Our results demonstrated that IFT80 plays an essential role in chondrocyte differentiation likely through regulating Hh/Gli and Wnt/α-catenin signal pathways.

Materials and methods

Cells and cell culture

Mouse BMSCs were isolated from a 6-week-old C57BL/J mouse and cultured in our laboratory as described previously [47]. All animal procedures were conducted in accordance with the protocol approved by the Institutional Animal Care and Use Committee (IACUC) of the University at Buffalo (UB). Briefly, the mouse was sacrificed by CO_2, and the femurs were dissected free from the surrounding soft tissue in a sterile hood. BMSCs were collected by flushing the diaphysis with phosphate-buffered saline (PBS) after resetting the metaphysis from both ends. The cells were maintained in modified Eagle's medium alpha (a-MEM) containing 10% fetal bovine serum. The cells were cultured in 100-mm culture dishes in a humidified, mixed environment of 37 °C and 5% CO_2. The basic media consisted of a 1:1 mixture of Dulbecco's modified Eagle's medium and Ham's F-12 medium containing 5% fetal bovine serum.

Lentiviral gene transfer

To identify the function of the IFT80 gene in the chondrogenic differentiation and chondrocyte signaling pathways, we used lentivirus-mediated mouse pLKO.1-IFT80 shRNA plasmids and control pLB-scrambled shRNA (Open Biosystems, Lafayette, CO) to package IFT80 recombinant lentivirus according to the manufacturer's instructions. Briefly, five individual vector pLKO.1-IFT80 shRNAs (I1, I2, I3, I4, and I5) and pLKO.1-scramble shRNA (pLB Control) were respectively co-transfected with the packaging plasmids, pCMV-Dr8.2 and pCMV-VSVG (Addgene, Cambridge, MA) [48] into HEK293T cells (ATCC) using calcium phosphate co-precipitation method. The medium was replaced with fresh complete growth media after co-transfection for 8 h. After 48–72 h, the lentiviral supernatant was harvested and the titer was determined by infecting HEK293T cells with serial dilutions of concentrated lentivirus in the presence of 4 μg/mL polybrene (Sigma). The viral supernatant was added to mouse BMSCs. Forty-eight hours after transfection; the cells were analyzed by Western blot and immunostaining to test the silencing efficiency. The lentiviruses from the I3 clone had the best silencing efficiency compared to the other clones (data not shown) and were used in the following experiments indicated as I3. The control was designated as pLB. For chondrogenic differentiation analysis, the infected cells were induced with chondrogenic medium for the indicated times based on different experiments. The chondrogenic medium was purchased from Promocell (Promocell, Heidelberg, Germany) which consisted of 10 μg/mL human transferrin (Roche Diagnostics, Indianapolis, IN), 3×10^{-8} M sodium selenite (Sigma, St. Louis, MO) and 10 μg/mL human recombinant insulin (Roche Diagnostics).

Production of recombinant retrovirus

Retroviral vector pBMN-Gli2 was constructed by inserting a full-length Gli2 cDNA (access no. NM_001081125) into the EcoRI and NotI sites of pBMN-I-GFP (Addgene, Cambridge, MA), and packaging was performed according to the protocol from Dr. Garry Nolan's laboratory at Stanford University. Briefly, retrovirus vectors pBMN-I-GFP (control vector) and pBMN-IFT80 were separately transfected into the Phoenix ecotropic packaging cell line by the $CaCl_2$ precipitation method [49]. Following transfection, the cells were placed in a 32 °C humidified incubator for 48 h (a temperature of 32 °C aids in stabilizing the virus). The medium containing the infectious virus was harvested and filtered through a 0.45 mm filter to eliminate any contaminating Phoenix-eco cells and used for titer assays and the infection of mouse BMSCs. GFP and Gli2 protein expression was confirmed by observing GFP^+ cells and performing immunostaining and Western blots [50]. Retroviruses carrying either Gli2 cDNA or pBMN-I-GFP were then used to infect 70% subconfluent proliferating mouse BMSCs in the presence of 8 μg/mL polybrene.

Immunocytochemistry

To visualize the cilia, the cells were seeded at 1×10^5 cells/well on 24-well plates and incubated overnight, followed by infection with lentivirus IFT80 shRNA and/or retrovirus pBMN-Gli2 for 24 h. The cells were sequentially induced with chondrogenic medium with 10% FBS for 3 days. After 48 h of serum starvation (without FBS), the cells were fixed with 100% ice-cold methanol for 10 min and washed 3 times with PBS. Fixed cells were blocked with 5% bovine serum albumin (BSA) in PBS for 60 min. The cells were then incubated with primary antibody diluted in PBS containing 1% BSA for 1 h. The primary antibodies used were as follows: anti-IFT80 antibody (Abnova, Walnut, CA. 1:500), anti-ARL13B (Sigma, 1:500), anti-γ tubulin (Sigma, 1:1000) and mouse monoclonal anti-acetylated tubulin antibody (Sigma, 1:1000). After washing 3 times in PBS, Alexa Fluor 488-, Alexa Fluor 568- or Alexa Fluor 647-(Invitrogen, Grand Island, NY) conjugated anti-rabbit or anti-mouse IgG was added in PBS with 1% BSA for 1 h. After the final wash, 6-diamidino-2-phenylindole (DAPI) (Sigma) was added and used as a counterstain for nuclei [50].

For immunofluorescence staining of tibia sections, isolated tibia from 8 week-old wild type C57BL/6 mice were fixed in 10% neutral buffered formalin for 24 h. Immunofluorescence analyses were performed on paraffin sections. The specimens were boiled for 20 min with Tris-EDTA buffer (10 mM Tris Base, 1 mM EDTA solution, 0.05% Tween 20, pH 9.0). Before staining with rabbit anti-IFT80 antibody (Abnova, Walnut, CA. 1:200), the specimens were incubate 1 h with 5% BSA and 10% goat serum in PBS. Sections were then washed with PBS and incubated with Alexa Fluor 488- conjugated goat anti-rabbit IgG (1:1000). DAPI was added after final wash and used as a counterstain for nuclei. The negative control was included with same condition by using rabbit serum instead of rabbit anti-IFT80 antibody to confirm that the immunostaining signals are genuine. All Fluorescence images were acquired using a Zeiss Axio imager microscope.

To determine the β-catenin translocation, BMSCs were treated with pLB (control vector) or I3 (IFT80 shRNA) for 24 h, followed by cultured in the chondrogenic medium with or without 100 ng/mL Wnt3a recombinant protein for 24 h. Then all cells were fixed in 4% paraformaldehyde in PBS and permeabilized with 0.1% Triton X-100. Immunostaining was performed using rabbit anti-β-catenin (1:800, Cell Signaling Technology, Beverly, MA) antibody. Fixed cells were then washed with PBS and incubated with Alexa Fluor 488-conjugated goat anti-rabbit IgG (1:1000). DAPI was used to indicate the nuclei.

Alcian blue staining

BMSCs were treated with pLB (control vector) or I3 (IFT80 shRNA) for 24 h, followed by infection with retrovirus pBMN-Gli2 for 24 h. The the infected cell were cultured in the chondrogenic medium for 21 days. The cells were washed twice with PBS, fixed with methanol at −20 °C for 2 min, stained with 0.1% Alcian blue 8Gx (Sigma) in 0.1 N HCl overnight, and rinsed repeatedly with distilled water. For quantitative analysis, each culture plate stained with Alcian blue was extracted with 150 μL of 6 M guanidine-HCl for 2 h at room temperature. The extracted dye was transferred to 96-well plates, and the optical density was measured at 620 nm.

RNA isolation and RT-PCR

BMSCs were infected with pLB (control vector) or I3 (IFT80 shRNA) and pBMN-Gli2 as described above. Then the infected cells were induced with the chondrogenic medium for 14 days. Total RNA was extracted from Chondrogenic medium-induced BMSCs, using TRIzol reagent (Invitrogen). Following ethanol precipitation, total RNA was applied to an RNase column (Qiagen, Venlo, Netherlands) for further purification and treated with DNase following the manufacturer's protocol. cDNA was synthesized from 1 μg total RNA using the SuperScript III reverse transcriptase kit (Invitrogen) in a final volume of 20 μL. Primers were designed with the IDT SCI primer design tool (Integrated DNA Technologies, San Diego, California). RT-PCR experiments were performed with a Bio-Rad C1000 thermal cycler (Bio-Rad, Hercules, CA). Sequence and product lengths for each primer pair were as follows: GAPDH (forward, 5′-ACCACAGTCCATGCCATCAC-3′; reverse, 5′-TCCACCA CCCTGTTGCTGTA-3′); collagen II (forward, 5′-GCGACTGTCCCTCG GAAAAACTGG-3′; reverse, 5′-TTGAGGTTGCCAGCCGCTTCG-3′, 239 bp); aggrecan (forward, 5′-ACCT GGGTGGATGCGGAGAGAC-3′; reverse, 5′-ACCAGGGAGCTGATCTCGTAGC GA-3′, 398 bp). The RT-PCR data were quantitatively analyzed by NIH ImageJ software (NIH, Bethesda, MD, USA) and normalized to GAPDH expression.

Western blot

The infected cells were induced with chondrocyte medium for 14 days and then lysed with NP40 buffer (1% NP-40, 0.15 M NaCl, 50 mM Tris, pH 8.0) containing protease inhibitor cocktail (Sigma, St. Louis, MO.). The cell lysates were centrifuged at 12,000*g* for 10 min at 4 °C, and the supernatants were stored at −80 °C. Protein quantitation was performed with BCA protein assay reagent (Pierce, Rockford, IL, USA). Equal amounts of protein from the different groups were denatured in sodium dodecyl sulfate (SDS) sample buffer and separated on 8–10% polyacrylamide-SDS gel based on the protein molecular weight. Proteins were transferred to polyvinylidene difluoride (PVDF) membrane in 25 mM Tris, 192 mM glycine, and 20% methanol. The blots were blocked with Tris-buffered saline (TBS; 20 mM Tris–HCl [pH 7.5] and 137 mM NaCl) containing 0.1% Tween20 and 3% dried milk powder. Rabbit polyclonal antibodies to collagen II (Abcam), Gli2 (Abcam), partial recombinant IFT80 (Abnova,) and rabbit monoclonal antibodies to GAPDH (Cell signaling technology) and β-catenin (Cell signaling technology, 9562) were used to detect the target proteins. The β-catenin antibody used here was designed to detect the total endogenous β-catenin expression. The antigen-antibody complexes were detected using horseradish peroxidase-conjugated donkey anti-rabbit IgG secondary antibodies (Sigma) and the enhanced chemiluminescence detection system, as recommended by the manufacturers. The blots were visualized and quantified using Fluor-S Multi-Imager and Multi-Analyst software (Bio-Rad) [51].

Reporter assay

To examine whether silencing IFT80 affects Hh signaling activity, 1×10^6 cells were transfected with 3 μg Gli-responsive luciferase reporter construct (8 × Gli-Luc) (kindly provide by Dr. Fernandez-Zapico [52]), and 0.6 μg pRL-TK Renilla luciferase (Promega, Madison, WI) as internal control, by Fugene HD transfection reagent (Promega, Madison, WI). Cells were induced with chondrogenic medium for 7 days, and then stimulated with 1mg/mL of recombinant mouse Sonic Hedgehog (Shh) N-terminus (R&D systems, Minneapolis, MN) for additional 8 h before assay [53]. The relative luciferase activity of cell lysates was measured by Veritas microplate luminometer (Turner Biosystem, Sunnyvale, CA) using a Dual-luciferase assay kit (Promega, Madison, WI).

To explore the potential effect of IFT80 silencing on Wnt signaling pathway, control (pLB) and IFT80-silenced (I3) BMSCs were transiently cotransfected with 3.0 μg M50 Super 8 × TOPFlash luciferase reporter plasmid (M508 × TOPFlash-Luc, Addgene, Cambridge, MA), or 3.0 μg M51 Super 8 × FOPFlash (TOPFlash mutant) and 0.6 μg pRL-TK Renilla luciferase (Promega, Madison, WI) as internal control, by Fugene HD Transfection Reagent. Cells were induced with chondrogenic medium for 7 days, and then induced with or without 100 ng/mL of recombinant Wnt3a (Applied stem cell, Menlo Park, CA) for additional 8 h [53]. The relative luciferase activity of cell lysates was measured by Veritas microplate luminometer (Turner Biosystem, Sunnyvale, CA) using a Dual-luciferase assay kit (Promega, Madison, WI)

Statistical analyses

Statistical analysis was performed using SPSS-17.0 software. Data were analyzed using one-way analysis of variance, and Tukey's HSD test was applied as a post hoc test if statistical significance was determined. Statistical significance for the two groups was assessed using Student's *t*-test. The probability level at which differences were considered significant was $P < 0.05$.

Results

IFT80 is prominently expressed in growth plate and during chondrocyte differentiation

To detect the expression pattern of IFT80, mouse tibia sections were stained with anti-IFT80 antibody as described in the Materials and methods section. Negative control was included in the same staining run to confirm that the immunostaining signals were genuine. We found that IFT80 was highly expressed in the growth plate as well as trabecular bone (Fig. 1A). Higher magnification images showed IFT80 expression in nearly all chondrocytes located in the growth plate (Fig. 1A). RT-PCR in BMSCs with a time course of chondrogenic induction showed that IFT80 mRNA expression was detected in BMSCs at day 0 and gradually increased and reached its peak at day 15 during the chondrogenic process and continuously expressed until mature chondrocytes at day 30 (Fig. 1B and C). These results indicate that IFT80 protein is expressed in early stages of chondrocytes, and it continues to be expressed throughout the entirety of differentiation.

Silencing IFT80 blocks cilia formation in mouse BMSCs

To study the function of IFT80 in cilia formation, we used lentivirus-based RNA interference (RNAi) technology to silence IFT80 expression in mouse BMSCs. After transfection with IFT80 shRNA constructs, we packaged the recombinant lentivirus carrying five constructs pLKO.1-IFT80 shRNAs (I1, I2, I3, I4, and I5) and pLKO.1-scramble shRNA (pLB Control). Mouse BMSCs were infected with these viruses for 48 h and then lysed for the analysis of IFT80 expression. The lentiviruses from the I3 clone had the best silencing

efficiency compared to the other clones (data not shown) and were used in the following experiments indicated as I3. The levels of IFT80 protein greatly decreased in I3-infected BMSCs compared to the pLB-infected group (pLB) (Fig. 2A). To identify the efficiency of IFT80 silencing and the subcellular distribution of the IFT80 protein, we used immunofluorescence staining to detect IFT80 protein expression in mouse BMSCs. Our results showed that the red fluorescence of IFT80 overlaps with the bright blue fluorescence of acetylated tubulin in the cilia in control cells but not in the IFT80-silenced cells (Fig. 2B). To further investigate the role of IFT80 in cilia formation, mouse BMSCs were infected by I3 and pLB for 48 h. The cilia were visualized by co-immunostaining for acetylated tubulin (bright blue), and/or γ-tubulin (red). As shown in Fig. 2C, about 70% BMSCs infected by pLB showed apparent cilia formation, while in IFT80-silenced group, only 15–20% BMSCs had cilia formation. These results demonstrates that IFT80 is required for cilia formation.

Silencing IFT80 impairs chondrocyte differentiation

To investigate whether IFT80 plays a role in chondrocyte differentiation, mouse BMSCs were infected as described in the Materials and methods section and then induced with chondrogenic medium for 21 days. Alcian blue staining was used to detect sulfated proteoglycan deposits, which are indicative of functional chondrocytes [54]. The results showed that IFT80 silencing inhibited chondrocyte differentiation (Fig. 3A, I3 panels). Quantification of the Alcian blue dyes showed a 43% decrease in the I3 group compared with the pLB group ($^{*}P < 0.05$) (Fig. 3B, pLB and I3 panels). The bright field microscopy images also shown the sulfated proteoglaycan deposits were significantly decreased in the I3 group and the cell morphology did not show difference (Fig. 3C). Additionally, immunostaining and western blot results showed a significant decrease in the expression level of chondrocyte marker gene collagen II in IFT80-silenced BMSCs compared with pLB control cells (Fig. 3D, Panels of pLB and I3, and Fig. 4C and D). Furthermore, RT-PCR further confirmed that silencing IFT80 significantly down-regulated the expression of collagen II and aggrecan (Fig. 4A and B). These results demonstrate that silencing IFT80 impaired chondrocyte differentiation and its marker genes expression.

Silencing IFT80 dampens the Hh signaling pathway activity

The above observations suggested that IFT80 is essential for chondrocyte differentiation. To gain further insight into the molecular mechanisms of IFT80 in chondrocyte differentiation, we hypothesized that the Hh signaling pathway is involved in this event. To test hypothesis, we first determine the effect of silencing IFT80 on Gli2 expression, which is a critical transcriptional factor in Hh signaling pathway [55]. Immunostaining (Fig. 3D) and Western blot results (Fig. 4C) showed a large decrease in Gli2 expression in IFT80-silenced cells (I3). To fully understand the involvement of Hh/Gli signaling in IFT80-mediated chondrogenic differentiation of BMSCs, we constructed a Gli2-overexpressing vector to ectopic express Gli2 in IFT80-silenced cells and control cells. Immunostaining (Fig. 3D, Gli2 panel) and Western blot (Fig. 4C, Gli2 panel) confirmed the overexpression of Gli2. Overexpressing Gli2 in IFT80-silenced cells (Fig. 3A–C, I3+Gli2 panel) dramatically increased the sulfated proteoglycan deposits, however the increase is less than that in Gli2-overexpressed control cells (Fig. 3A–C, Gli2 panel, $^{\#}p < 0.05$). Moreover, the expression of collagen II was restored by the overexpression of Gli2 in IFT80-silenced BMSCs (Fig. 3D). This result was further confirmed by RT-PCR (Fig. 4A and B) and Western blot (Fig. 4C and D). In addition to collagen II, RT-PCR data also showed overexpression of Gli2 in IFT80-silenced BMSCs rescued aggrecan expression (Fig. 4A). Collectively, these results demonstrate that overexpression of Gli2 promotes chondrocyte differentiation in normal cells and rescues the deficiency of chondrocyte differentiation from IFT80 silencing. These results also suggest that IFT80 likely acts upstream of Gli2 signaling.

To elucidate the effect of IFT80 on Hh signaling activity, we performed a dual-luciferase activity assay with p8 × Gli-Luc construct [53]. The pLB and I3 infected BMSC cells were induced with the chondrogenic medium for 7 days and then stimulated with 1 μg/mL Shh for additional 8 h. The result showed that addition of Shh to control cells (BMSCs treated with pLB) resulted in a significant increase in Gli-responsive-promoter luciferase activity compared to that without Shh stimulation. In agreement with the decreases of Gli2 expression in IFT80-silenced cells described above, Shh-induced Gli-responsive-promoter luciferase activity in IFT80-silenced cells was significantly lower than that in control cells (Fig. 4E), indicating that silencing IFT80 attenuates Hh signaling activity in chondrocyte differentiation.

Silencing IFT80 promotes theWnt/β-catenin signaling activity

To determine the role of IFT80 in regulating Wnt signaling activity, a dual-luciferase assay using Super 8 × TOPFlash construct was performed [53]. The transfected BMSC cells were induced with the chondrogenic medium for 7 days and then stimulated with 100 ng/mL Wnt3a recombinant protein for additional 8 h to activate the Wnt signaling pathway. The result showed that the induction of Wnt3a led to a 9-fold increase in Super 8 × TOPFlash promoter luciferase activity in control BMSCs, and a 13-fold increase in IFT80-silenced cells (Fig. 5A). Besides, without Wnt3a induction, IFT80-silenced cells showed higher Super 8xTOPFlash promoter luciferase activity than the control cells (Fig. 5A). These results suggested that silencing IFT80 promotes Wnt signaling activity.

To further confirm the role of IFT80 in Wnt/β-catenin signaling pathway, we detected the expression levels of Wnt downstream effector: β-catenin. We found that β-catenin was highly up-regulated in IFT80-silenced BMSCs compared with the control group (Fig. 5B and C). We next examined the subcellular localization of β-catenin. Interestingly, we observed that the absence of Wnt ligand, β-catenin proteins accumulated in cytosol in the control cells, however, in the IFT80-silenced cells, β-catenin proteins localized in cell nucleus (Fig. 5D). Furthermore, when stimulated with 100 ng/mL Wnt3a recombinant protein, both IFT80-silenced and control cells exhibited nuclear translocation of β-catenin (Fig. 5E). These results indicated that IFT80 restricts Wnt/β-catenin signaling activity.

Discussion

IFT80 partial mutations in humans cause JATD [44] and SRP syndrome type III [46]. These diseases are autosomal recessive chondrodysplasias characterized by shortening of the long bones and constriction of the thoracic cage. However, it is unknown if the abnormal skeletal phenotypes are resulted from indirect effect of mutation of IFT80 in human tissues or due to the effect of IFT80 mutation on chondrogenic differentiation. Therefore, in this study, our aim is to elucidate the role of IFT80 in cilia formation and chondrocyte differentiation and to identify the pathways involved in this progress. Our study has shown that IFT80 was highly expressed in the mouse growth plate and during chondrocyte differentiation. Silencing IFT80 abolished cilia assembly, which is consistent with previous reports that mutation of IFT80 shortens the cilia or impairs the growth of cilia in tetrahymena thermophile [44], *Chlamydomonas reinhardtii* [56] and mouse models [57]. We also found that silencing IFT80 impairs chondrocyte differentiation in BMSCs by inhibiting the expression of the chondrocyte-specific genes collagen II and aggrecan and regulating Hh signaling and Wnt signaling pathways. While the regulation of the IFT80 protein has been primarily studied in osteoblasts [58], polydactyly syndromes in mouse [57], and photoreceptor cell death in zebrafish [45], this report is the first to demonstrate that IFT80 is involved in the regulation of chondrogenic differentiation.

Many studies have demonstrated a clear relationship between cilia and cell differentiation, or cell lineage determination [59–61]. The study of the OA and cilia has revealed the cilia are involved in the terminal differentiation of chondrocytes [23]. Tummala et al. reported that primary cilia in human BMSCs are necessary for chemically induced osteogenic, adipogenic, and chondrogenic differentiation [61]. The loss of cilia in BMSCs leads to decreased expression of the chondrogenic marker gene SOX9 and impaired chondrogenic differentiation [61]. In agreement with these findings, our results showed that silencing IFT80 led to the loss of cilia and the impaired chondrocyte differentiation. Additionally, the expression of the chondrocyte marker genes aggrecan and collagen II decreased in IFT80-silenced cells. These results suggested that IFT80 plays an essential role in cilia formation and chondrocyte differentiation.

It have been reported that IFT proteins play critical roles in primary cilia assembly and Hh signaling pathway [9,11,30,31,62]. Recently, Rix et al. generated a murine IFT80 gene-trap line. They found that hypomorphic levels of IFT80 result in more than 97% embryonic lethality and a significant reduction in Hh pathway activation in response to Hh analog treatment in mouse embryonic fibroblasts [57], suggesting that IFT80 is involved in regulating the Hh/Gli signaling pathway. In consistent with those findings, we found that silencing IFT80 impaired chondrocyte differentiation, and significantly decreased Gli2 expression and the Gli-responsive-promoter luciferase activity. Moreover, chondrogenic deficiency in IFT80-silenced cells could be rescued by the overexpression of Gli2. It is worth mentioning that in IFT80 gene-trap mouse model, partial deletion of IFT80 with a lower level of IFT80 defects Hh signaling pathway, but does not affect the cilia formation [57]. However, our results showed that silencing IFT80 in BMSCs disrupted cilia formation. One possible explanation for this inconsistence is that a very low level or loss of IFT80 blocks cilia formation; however, if IFT80 exists and reaches a certain level, transporting function of IFT would not be affected, and thus cilia formation can be maintained normally. Most recently, Keady et al. found that IFT25, another member of IFT complex B, is not required for ciliary assembly, but deletion of IFT25 does cause major defects in Shh signaling and display phenotypes indicative of aberrant Shh signaling [11]. This study suggests that there are two possibilities for IFT80 to regulate Hh signaling pathway. One is that IFT80 secondarily affects Hh signaling due to loss of cilia, and the other is that IFT80 directly regulates Hh signaling pathway in ciliary independent manner.

The Wnt signaling pathway is another important pathway involved in bone development and chondrocyte differentiation [63]. IFT proteins have been implicated in restraining the canonical Wnt pathway [43,64–67]. β-catenin is a transcription factor, which is activated and increased in the presence of Wnt in the canonical Wnt signaling pathway [68]. In this study, silencing IFT80 increased the expression level of β-catenin, β-catenin nuclear translocation and β-catenin reporter luciferase activity, suggesting that IFT80 negatively regulates the Wnt signaling pathway in BMSCs. Most recently, Chang et al. reported that *Sfrp*5, extracellular antagonist of Wnt signaling, is a downstream target of Hh in rib chondrocytes [67]. This finding suggests a potential crosstalk between Wnt and Hh signaling pathways. Since silencing IFT80 also inhibits the Hh signaling pathway and up-regulates Wnt signaling pathway, in the further study it would be interesting to reveal the relationship of Hh and Wnt signaling pathways by which IFT80 regulates in chondrocyte differentiation.

Overall, our findings implicate the role of IFT80 in chondrocyte differentiation and provide direct evidence for IFT80 regulation in the Hh and Wnt/β-catenin signaling pathways. Most recently, McIntyre [69] et al. found that adenoviral-mediated expression of IFT88 can restore ciliary structures and rescue olfactory function in IFT88 mutant mice. This study provides a proof and an effective therapeutic option by using IFT proteins to rescue of the complex ciliary organelle in IFT/Cilia and Hh signaling related human diseases. Elucidation

of the role and mechanism of IFT80 can provide novel gene therapeutic targets for treatment of JATD, SRPIII and other diseases.

Acknowledgments

We thank Dr. Elizabeth (Betty) A. Smith and David Hadbawnik for critical reading of the manuscript and Dr. Wade J. Sigurdson, the director of the Confocal Microscope Facility at the School of Medicine and Biomedical Sciences, University at Buffalo, for assistance with fluorescence microscopy. This work was supported by a National Institute of Health grant AR055678 (S. Yang) and AR061052 (S. Yang).

Abbreviations

JATD	Jeune asphyxiating thoracic dystrophy
SRP	Short-rib polydactyly
OA	Osteoarthritis
IFT	Intraflagellar transport
Ptch1	Patched 1
Smo	Smoothened
Hh	Hedgehog
Shh	Sonic Hh
shRNA	Small hairpin RNA
BMSC	Bone marrow-derived stromal cells
PBS	Phosphate-buffered saline
DAPI	Propidium iodide (PI) 6-diamidino-2-phenylindole
SDS	Sodium dodecyl sulfate
PVDF	Polyvinylidene difluoride
RNAi	RNA interference
IL-1	Interleukin-1
BSA	Bovine serum albumin

REFERENCES

1. Berbari NF, O'Connor AK, Haycraft CJ, Yoder BK. The primary cilium as a complex signaling center. Curr. Biol. 2009; 19:R526–R535. [PubMed: 19602418]
2. Ishikawa H, Marshall WF. Ciliogenesis: building the cell's antenna. Nat. Rev. Mol. Cell Biol. 2011; 12:222–234. [PubMed: 21427764]
3. Satir P, Christensen ST. Overview of structure and function of mammalian cilia. Annu. Rev. Physiol. 2007; 69:377–400. [PubMed: 17009929]
4. Takeda S, Narita K. Structure and function of vertebrate cilia, towards a new taxonomy. Differentiation. 2012; 83:S4–S11. [PubMed: 22118931]
5. Pedersen LB, Rosenbaum JL. Intraflagellar transport (IFT) role in ciliary assembly, resorption and signalling. Curr. Top. Dev. Biol. 2008; 85:23–61. [PubMed: 19147001]
6. Pazour GJ, Dickert BL, Vucica Y, Seeley ES, Rosenbaum JL, Witman GB, Cole DG. Chlamydomonas IFT88 and its mouse homologue, polycystic kidney disease gene tg737, are required for assembly of cilia and flagella. J. Cell Biol. 2000; 151:709–718. [PubMed: 11062270]
7. Gorivodsky M, Mukhopadhyay M, Wilsch-Braeuninger M, Phillips M, Teufel A, Kim C, Malik N, Huttner W, Westphal H. Intraflagellar transport protein 172 is essential for primary cilia formation

and plays a vital role in patterning the mammalian brain. Dev. Biol. 2009; 325:24–32. [PubMed: 18930042]

8. Moyer JH, Lee-Tischler MJ, Kwon HY, Schrick JJ, Avner ED, Sweeney WE, Godfrey VL, Cacheiro NL, Wilkinson JE, Woychik RP. Candidate gene associated with a mutation causing recessive polycystic kidney disease in mice. Science. 1994; 264:1329–1333. [PubMed: 8191288]
9. Huangfu D, Liu A, Rakeman AS, Murcia NS, Niswander L, Anderson KV. Hedgehog signalling in the mouse requires intraflagellar transport proteins. Nature. 2003; 426:83–87. [PubMed: 14603322]
10. Cole BR, Conley SB, Stapleton FB. Polycystic kidney disease in the first year of life. J. Pediatr. 1987; 111:693–699. [PubMed: 3668738]
11. Keady BT, Samtani R, Tobita K, Tsuchya M, San Agustin JT, Follit JA, Jonassen JA, Subramanian R, Lo CW, Pazour GJ. IFT25 links the signal-dependent movement of Hedgehog components to intraflagellar transport. Dev. Cell. 2012; 22:940–951. [PubMed: 22595669]
12. Wang Z, Fan ZC, Williamson SM, Qin H. Intraflagellar transport (IFT) protein IFT25 is a phosphoprotein component of IFT complex B and physically interacts with IFT27 in *Chlamydomonas* . PloS One. 2009; 4:e5384. [PubMed: 19412537]
13. Qin H, Wang Z, Diener D, Rosenbaum J. Intraflagellar transport protein 27 is a small G protein involved in cell-cycle control. Curr. Biol. 2007; 17:193–202. [PubMed: 17276912]
14. Wilsman NJ. Cilia of adult canine articular chondrocytes. J. Ultrastruct. Res. 1978; 64:270–281. [PubMed: 712881]
15. Scherft JP, Daems WT. Single cilia in chondrocytes. J. Ultrastruct. Res. 1967; 19:546–555. [PubMed: 6055783]
16. Poole CA, Jensen CG, Snyder JA, Gray CG, Hermanutz VL, Wheatley DN. Confocal analysis of primary cilia structure and colocalization with the Golgi apparatus in chondrocytes and aortic smooth muscle cells. Cell Biol. Int. 1997; 21:483–494. [PubMed: 9451805]
17. Jensen CG, Poole CA, McGlashan SR, Marko M, Issa ZI, Vujcich KV, Bowser SS. Ultrastructural, tomographic and confocal imaging of the chondrocyte primary cilium in situ. Cell Biol. Int. 2004; 28:101–110. [PubMed: 14984755]
18. Wann AK, Zuo N, Haycraft CJ, Jensen CG, Poole CA, McGlashan SR, Knight MM. Primary cilia mediate mechanotransduction through control of ATP-induced Ca2+ signaling in compressed chondrocytes. FASEB J.: Off. Publ. Fed. Am. Soc. Exp. Biol. 2012; 26:1663–1671.
19. McGlashan SR, Knight MM, Chowdhury TT, Joshi P, Jensen CG, Kennedy S, Poole CA. Mechanical loading modulates chondrocyte primary cilia incidence and length. Cell Biol. Int. 2010; 34:441–446. [PubMed: 20100169]
20. Song B, Haycraft CJ, Seo HS, Yoder BK, Serra R. Development of the post-natal growth plate requires intraflagellar transport proteins. Dev. Biol. 2007; 305:202–216. [PubMed: 17359961]
21. Muhammad H, Rais Y, Miosge N, Ornan EM. The primary cilium as a dual sensor of mechanochemical signals in chondrocytes. Cell Mol. Life Sci. 2012; 69:2101–2107. [PubMed: 22241332]
22. Chen X, Macica CM, Nasiri A, Broadus AE. Regulation of articular chondrocyte proliferation and differentiation by indian hedgehog and parathyroid hormone-related protein in mice. Arthritis Rheum. 2008; 58:3788–3797. [PubMed: 19035497]
23. McGlashan SR, Cluett EC, Jensen CG, Poole CA. Primary cilia in osteoarthritic chondrocytes: from chondrons to clusters. Dev. Dyn. 2008; 237:2013–2020. [PubMed: 18330928]
24. Wann AK, Knight MM. Primary Cilia Elongation in Response to Interleukin-1 Mediates the Inflammatory Response. Cellular and Molecular Life Sciences: CMLS. 2012
25. Merrill AE, Merriman B, Farrington-Rock C, Camacho N, Sebald ET, Funari VA, Schibler MJ, Firestein MH, Cohn ZA, Priore MA, Thompson AK, Rimoin DL, Nelson SF, Cohn DH, Krakow D. Ciliary abnormalities due to defects in the retrograde transport protein DYNC2H1 in short-rib polydactyly syndrome. Am. J. Hum. Genet. 2009; 84:542–549. [PubMed: 19361615]
26. Song JK, Niimi Y, Kupersmith MJ, Berenstein A. Postnatal growth and development of a cerebral arteriovenous malformation on serial magnetic resonance imaging in a child with hemangiomatosis. Case report. J Neurosurg. 2007; 106:384–387. [PubMed: 17566206]

27. Kinumatsu T, Shibukawa Y, Yasuda T, Nagayama M, Yamada S, Serra R, Pacifici M, Koyama E. TMJ development and growth require primary cilia function. J. Dent. Res. 2011; 90:988–994. [PubMed: 21566205]
28. Shao YY, Wang L, Welter JF, Ballock RT. Primary cilia modulate Ihh signal transduction in response to hydrostatic loading of growth plate chondrocytes. Bone. 2012; 50:79–84. [PubMed: 21930256]
29. Chang CF, Ramaswamy G, Serra R. Depletion of primary cilia in articular chondrocytes results in reduced Gli3 repressor to activator ratio, increased Hedgehog signaling, and symptoms of early osteoarthritis Osteoarthritis and cartilage/OARS. Osteoarthritis Res. Soc. 2012; 20:152–161.
30. Eggenschwiler JT, Anderson KV. Cilia and developmental signaling. Annu. Rev. Cell Dev. Biol. 2007; 23:345–373. [PubMed: 17506691]
31. Ocbina PJ, Anderson KV. Intraflagellar transport, cilia, and mammalian Hedgehog signaling: analysis in mouse embryonic fibroblasts. Dev. Dyn. 2008; 237:2030–2038. [PubMed: 18488998]
32. Koyama E, Young B, Nagayama M, Shibukawa Y, Enomoto-Iwamoto M, Iwamoto M, Maeda Y, Lanske B, Song B, Serra R, Pacifici M. Conditional Kif3a ablation causes abnormal hedgehog signaling topography, growth plate dysfunction, and excessive bone and cartilage formation during mouse skeletogenesis. Development. 2007; 134:2159–2169. [PubMed: 17507416]
33. St-Jacques B, Hammerschmidt M, McMahon AP. Indian hedgehog signaling regulates proliferation and differentiation of chondrocytes and is essential for bone formation. Genes Dev. 1999; 13:2072–2086. [PubMed: 10465785]
34. Hui CC, Angers S. Gli proteins in development and disease. Annu. Rev. Cell Dev. Biol. 2011; 27:513–537. [PubMed: 21801010]
35. Singla V, Reiter JF. The primary cilium as the cell's antenna: signaling at a sensory organelle. Science. 2006; 313:629–633. [PubMed: 16888132]
36. Jiang J, Hui CC. Hedgehog signaling in development and cancer. Dev. Cell. 2008; 15:801–812. [PubMed: 19081070]
37. Varjosalo M, Taipale J. Hedgehog: functions and mechanisms. Genes Dev. 2008; 22:2454–2472. [PubMed: 18794343]
38. Cadigan KM, Nusse R. Wnt signaling: a common theme in animal development. Genes Dev. 1997; 11:3286–3305. [PubMed: 9407023]
39. Wodarz A, Nusse R. Mechanisms of Wnt signaling in development. Annu. Rev. Cell Dev. Biol. 1998; 14:59–88. [PubMed: 9891778]
40. Tamamura Y, Otani T, Kanatani N, Koyama E, Kitagaki J, Komori T, Yamada Y, Costantini F, Wakisaka S, Pacifici M, Iwamoto M, Enomoto-Iwamoto M. Developmental regulation of Wnt/beta-catenin signals is required for growth plate assembly, cartilage integrity, and endochondral ossification. J. Biol. Chem. 2005; 280:19185–19195. [PubMed: 15760903]
41. Yuasa T, Kondo N, Yasuhara R, Shimono K, Mackem S, Pacifici M, Iwamoto M, Enomoto-Iwamoto M. Transient activation of Wnt/{beta}-catenin signaling induces abnormal growth plate closure and articular cartilage thickening in postnatal mice. Am. J. Pathol. 2009; 175:1993–2003. [PubMed: 19815716]
42. Corbit KC, Shyer AE, Dowdle WE, Gaulden J, Singla V, Chen MH, Chuang PT, Reiter JF. Kif3a constrains beta-catenindependent Wnt signalling through dual ciliary and non-ciliary mechanisms. Nat. Cell Biol. 2008; 10:70–76. [PubMed: 18084282]
43. He X. Cilia put a brake on Wnt signalling. Nat. Cell Biol. 2008; 10:11–13. [PubMed: 18172427]
44. Beales PL, Bland E, Tobin JL, Bacchelli C, Tuysuz B, Hill J, Rix S, Pearson CG, Kai M, Hartley J, Johnson C, Irving M, Elcioglu N, Winey M, Tada M, Scambler PJ. IFT80, which encodes a conserved intraflagellar transport protein, is mutated in Jeune asphyxiating thoracic dystrophy. Nat. Genet. 2007; 39:727–729. [PubMed: 17468754]
45. Hudak LM, Lunt S, Chang CH, Winkler E, Flammer H, Lindsey M, Perkins BD. The intraflagellar transport protein ift80 is essential for photoreceptor survival in a zebrafish model of jeune asphyxiating thoracic dystrophy. Invest. Ophthalmol. Vis. Sci. 2010; 51:3792–3799. [PubMed: 20207966]
46. Cavalcanti DP, Huber C, Sang KH, Baujat G, Collins F, Delezoide AL, Dagoneau N, Le Merrer M, Martinovic J, Mello MF, Vekemans M, Munnich A, Cormier-Daire V. Mutation in IFT80 in a

fetus with the phenotype of Verma-Naumoff provides molecular evidence for Jeune-Verma-Naumoff dysplasia spectrum. J. Med. Genet. 2011; 48:88–92. [PubMed: 19648123]

47. He X, Dziak R, Mao K, Genco R, Swithart M, Li C, Yang S. Integration of a novel injectable nano calcium sulfate/alginate scaffold and BMP2 gene-modified mesenchymal stem cells for bone regeneration. Tissue Eng. Part A. 2012
48. Stewart SA, Dykxhoorn DM, Palliser D, Mizuno H, Yu EY, An DS, Sabatini DM, Chen IS, Hahn WC, Sharp PA, Weinberg RA, Novina CD. Lentivirus-delivered stable gene silencing by RNAi in primary cells. RNA. 2003; 9:493–501. [PubMed: 12649500]
49. Yang S, Li YP. RGS10-null mutation impairs osteoclast differentiation resulting from the loss of $[Ca^{2+}]$i oscillation regulation. Genes Dev. 2007; 21:1803–1816. [PubMed: 17626792]
50. Yang S, Li YP. RGS12 is essential for RANKL-evoked signaling for terminal differentiation of osteoclasts in vitro. J. Bone Miner. Res. 2007; 22:45–54. [PubMed: 17042716]
51. Wang W, Olson D, Liang G, Franceschi RT, Li C, Wang B, Wang SS, Yang SS. Collagen XXIV (Col24alpha1) promotes osteoblastic differentiation and mineralization through TGF-beta/Smads signaling pathway. Int. J. Biol. Sci. 2012; 8:1310–1322. [PubMed: 23139630]
52. Kurita S, Mott JL, Almada LL, Bronk SF, Werneburg NW, Sun SY, Roberts LR, Fernandez-Zapico ME, Gores GJ. GLI3-dependent repression of DR4 mediates hedgehog antagonism of TRAIL-induced apoptosis. Oncogene. 2010; 29:4848–4858. [PubMed: 20562908]
53. Qiu N, Xiao Z, Cao L, Buechel MM, David V, Roan E, Quarles LD. Disruption of Kif3a in osteoblasts results in defective bone formation and osteopenia. J. Cell Sci. 2012; 125:1945–1957. [PubMed: 22357948]
54. Kistler A, Tsuchiya T, Tsuchiya M, Klaus M. Teratogenicity of arotinoids (retinoids) in vivo and in vitro. Arch. Toxicol. 1990; 64:616–622. [PubMed: 2090029]
55. Kim J, Kato M, Beachy PA. Gli2 trafficking links Hedgehog-dependent activation of Smoothened in the primary cilium to transcriptional activation in the nucleus. Proc. Nat. Acad. Sci. U.S.A. 2009; 106:21666–21671.
56. Dutcher SK, Li L, Lin H, Meyer L, Giddings TH Jr, Kwan AL, Lewis BL. Whole-genome sequencing to identify mutants and polymorphisms in *Chlamydomonas reinhardtii* . G3 (Bethesda). 2012; 2:15–22. [PubMed: 22384377]
57. Rix S, Calmont A, Scambler PJ, Beales PL. An Ift80 mouse model of short rib polydactyly syndromes shows defects in hedgehog signalling without loss or malformation of cilia. Hum. Mol. Genet. 2011; 20:1306–1314. [PubMed: 21227999]
58. Yang S, Wang C. The intraflagellar transport protein IFT80 is required for cilia formation and osteogenesis. Bone. 2012; 51:407–417. [PubMed: 22771375]
59. Ezratty EJ, Stokes N, Chai S, Shah AS, Williams SE, Fuchs E. A role for the primary cilium in Notch signaling and epidermal differentiation during skin development. Cell. 2011; 145:1129–1141. [PubMed: 21703454]
60. Irigoin F, Badano JL. Keeping the balance between proliferation and differentiation: the primary cilium. Curr. Genomics. 2011; 12:285–297. [PubMed: 22131874]
61. Tummala P, Arnsdorf EJ, Jacobs CR. The role of primary cilia in mesenchymal stem cell differentiation: a pivotal switch in guiding lineage commitment. Cell. Mol. Bioeng. 2010; 3:207–212. [PubMed: 20823950]
62. Ashe A, Butterfield NC, Town L, Courtney AD, Cooper AN, Ferguson C, Barry R, Olsson F, Liem KF Jr, Parton RG, Wainwright BJ, Anderson KV, Whitelaw E, Wicking C. Mutations in mouse Ift144 model the craniofacial, limb and rib defects in skeletal ciliopathies. Hum. Mol. Genet. 2012; 21:1808–1823. [PubMed: 22228095]
63. Maeda K, Takahashi N, Kobayashi Y. Roles of Wnt signals in bone resorption during physiological and pathological states. J. Mol. Med. (Berl). 2012
64. Clevers H. Wnt/beta-catenin signaling in development and disease. Cell. 2006; 127:469–480. [PubMed: 17081971]
65. Mak KK, Chen MH, Day TF, Chuang PT, Yang Y. Wnt/beta-catenin signaling interacts differentially with Ihh signaling in controlling endochondral bone and synovial joint formation. Development. 2006; 133:3695–3707. [PubMed: 16936073]

66. Church V, Nohno T, Linker C, Marcelle C, Francis-West P. Wnt regulation of chondrocyte differentiation. J. Cell Sci. 2002; 115:4809–4818. [PubMed: 12432069]

67. Chang CF, Serra R. Ift88 regulates hedgehog signaling, Sfrp5 expression, and beta-catenin activity in post-natal growth plate. J. Orthop. Res. 2012

68. Mosimann C, Hausmann G, Basler K. Beta-catenin hits chromatin: regulation of Wnt target gene activation. Nat. Rev. Mol. Cell Biol. 2009; 10:276–286. [PubMed: 19305417]

69. McIntyre JC, Davis EE, Joiner A, Williams CL, Tsai IC, Jenkins PM, McEwen DP, Zhang L, Escobado J, Thomas S, Szymanska K, Johnson CA, Beales PL, Green ED, Mullikin JC, Sabo A, Muzny DM, Gibbs RA, Attie-Bitach T, Yoder BK, Reed RR, Katsanis N, Martens JR. Gene therapy rescues cilia defects and restores olfactory function in a mammalian ciliopathy model. Nat. Med. 2012; 18:1423–1428. [PubMed: 22941275]

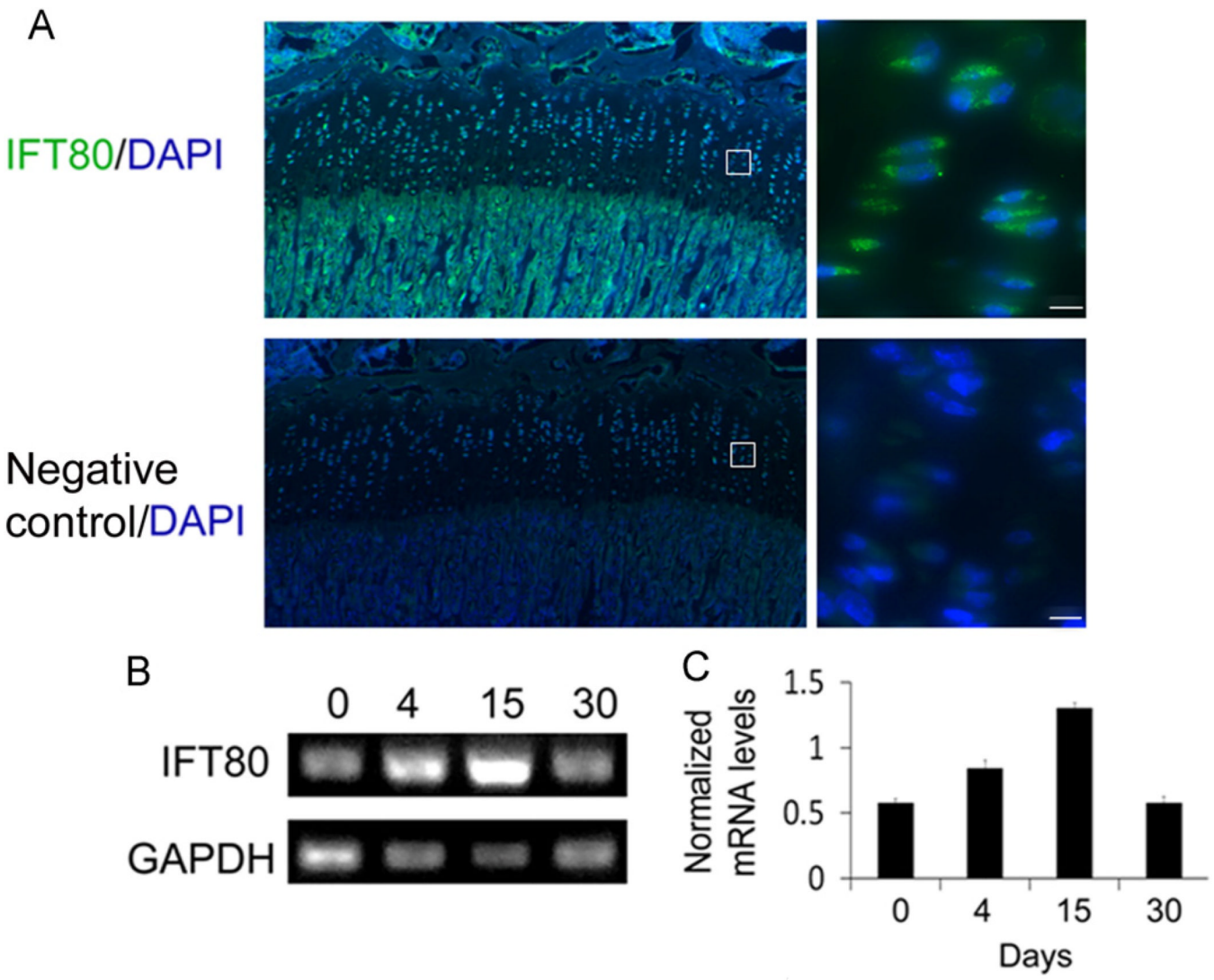

Fig. 1.

Expression pattern of IFT80. (A) Immunofluorescence staining analysis of IFT80 in the mouse tibia. Tibial section of mouse (8 weeks old) was stained with anti-IFT80 antibody (IFT80, green) or rabbit serum (negative control) and the nuclei were labeled with DAPI (DAPI, blue). (B) RT-PCR data showing the mRNA expression levels of IFT80 during the chondrogenic differentiation of BMSCs by induction with chondrogenic media for 0, 4, 15 and 30 days, respectively. (C) Quantitative analysis of IFT80 mRNA levels by normalization with GAPDH gene expression. The bars represent the means ±SEM, $N = 3$, $^{*}P < 0.05$: between each of two time points. The scale bar indicated 5 μm.

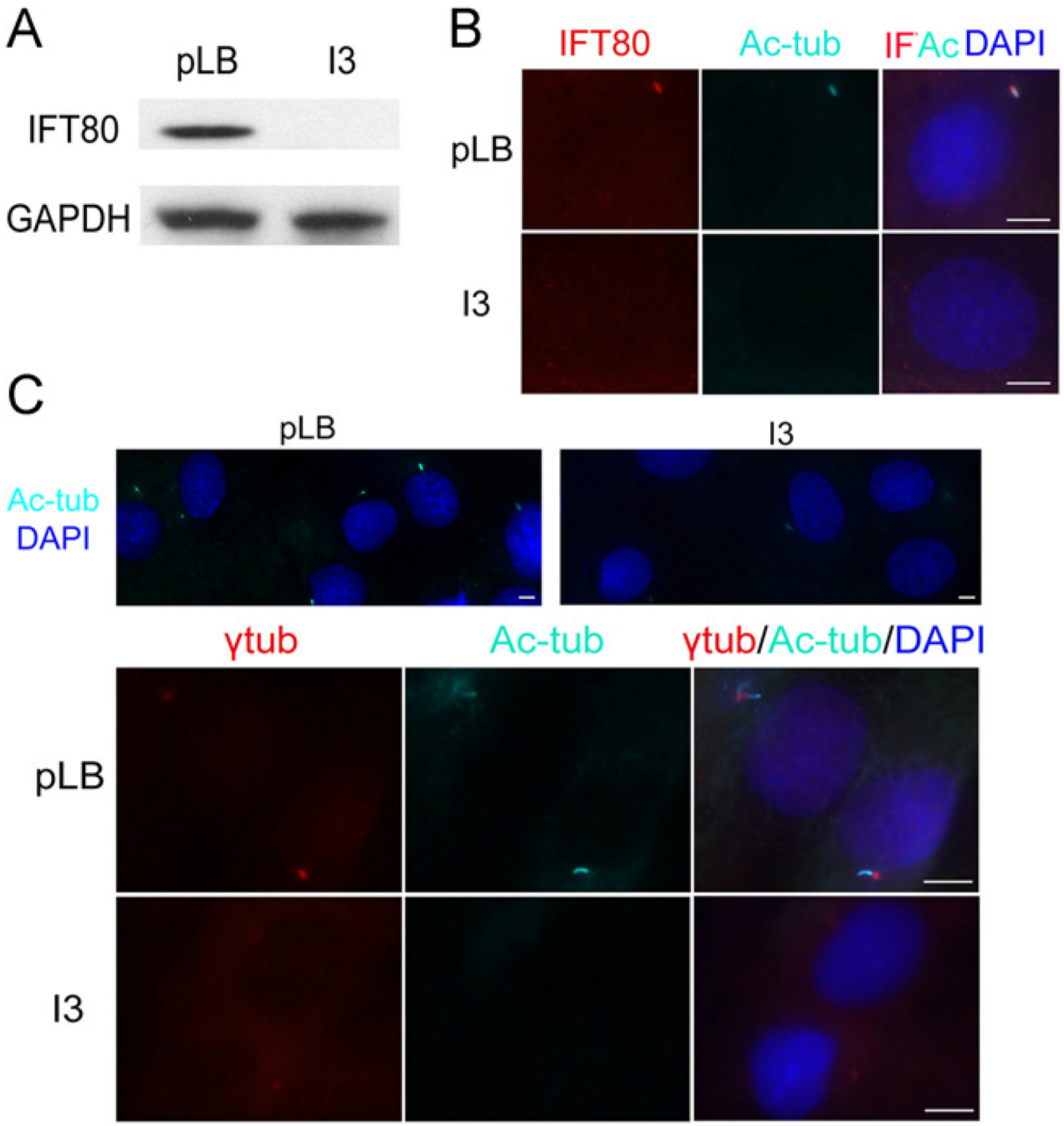

Fig. 2.

Silencing IFT80 impairs cilia formation. (A) Western blot validation of IFT80 expression in BMSCs infected with pLB and I3 for 48 h. GAPDH was used as a loading control. (B) Immunofluorescence staining for mouse BMSCs infected with pLB or I3 for 48 h. The cells were stained with anti-IFT80 (IFT80, red) and anti-acetylated tubulin (Ac-tub, bright blue). The nuclei were labeled with DAPI (DAPI, dark blue). The cells were imaged on a Zeiss Axioimager microscope (100×). (C) Immunostaining staining for mouse BMSCs infected with pLB or I3 for 48 h using anti-γ tubulin (γtub, red) and anti-acetylated tubulin (Ac-tub, bright blue). The nuclei were labeled with DAPI (DAPI, dark blue). The cells were imaged on a Zeiss Axioimager microscope (40× and QUOTE 100×). The scale bar indicated 5 μm.

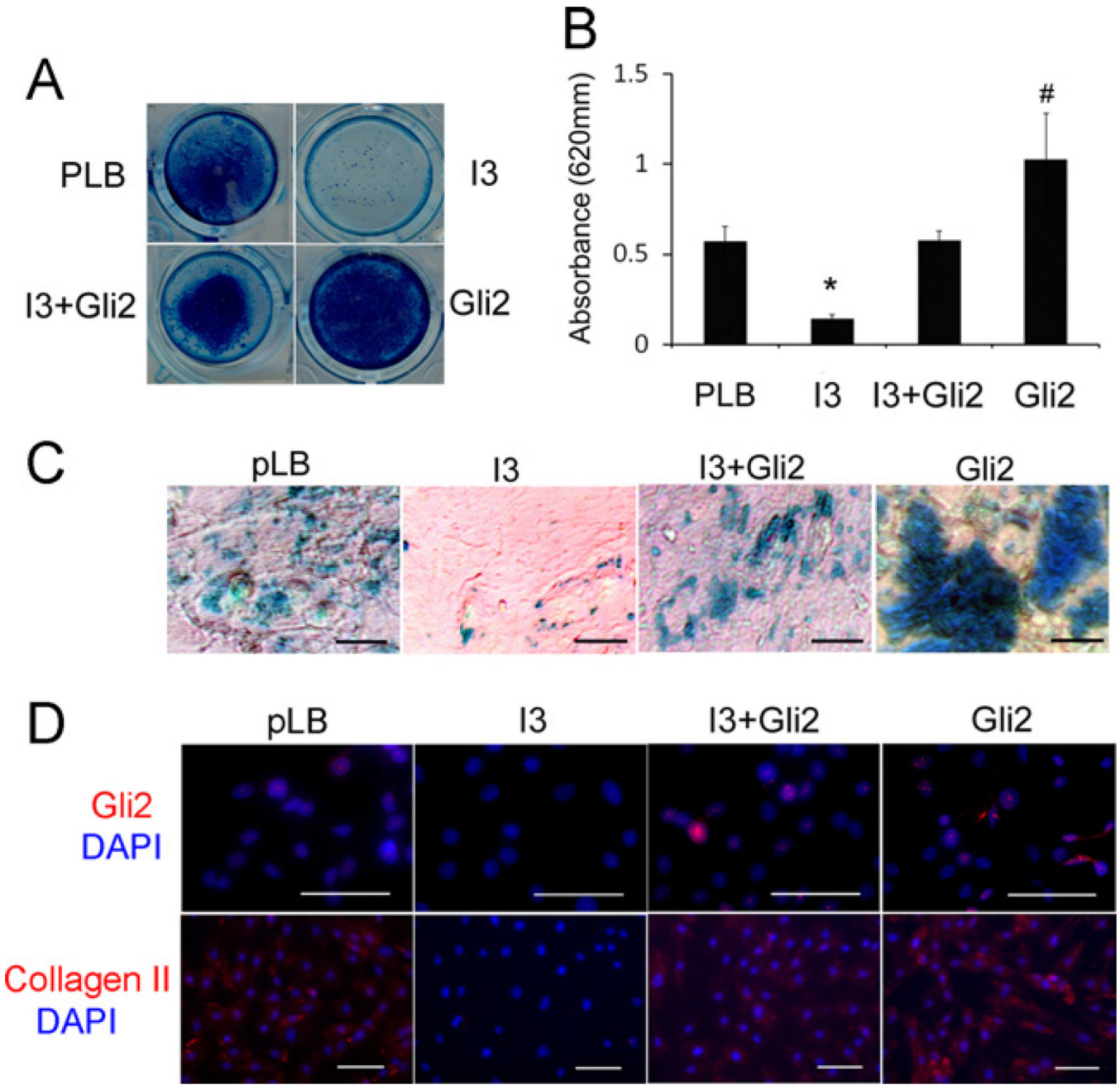

Fig. 3.

Silencing IFT80 impairs chondrocyte differentiation which was rescued by overexpression of Gli2. (A) Proteoglycan production was assessed by Alcian blue staining at day 21 after chondrogenic induction. Mouse BMSCs were infected with pLB and pBMN control (pLB), I3+pBMN control (I3), I3 with pBMN-Gli2 (I3+Gli2) or pBMN-Gli2+pLB (Gli2). (B) Quantitative assessment of Alcian blue staining by measuring the optical density of the dyes extracted by 6 M guanidine-HCl from different groups shown in A. Data represent the mean ±SEM. $N = 6$. $^{*}P < 0.001$, I3 vs. pLB, I3+Gli2 or Gli2. $^{\#}P < 0.05$, Gli2 vs. pLB, I3 or I3+Gli2. (C) Light filed microscopy image of the cells stained with Alcian blue at day 21 after chondrogenic induction. (D) Immunofluorescence of mouse BMSCs stained with anti-

Gli2 (Gli2, red) and anti-collagen II (Collagen II, red). The nuclei were labeled with DAPI (blue).

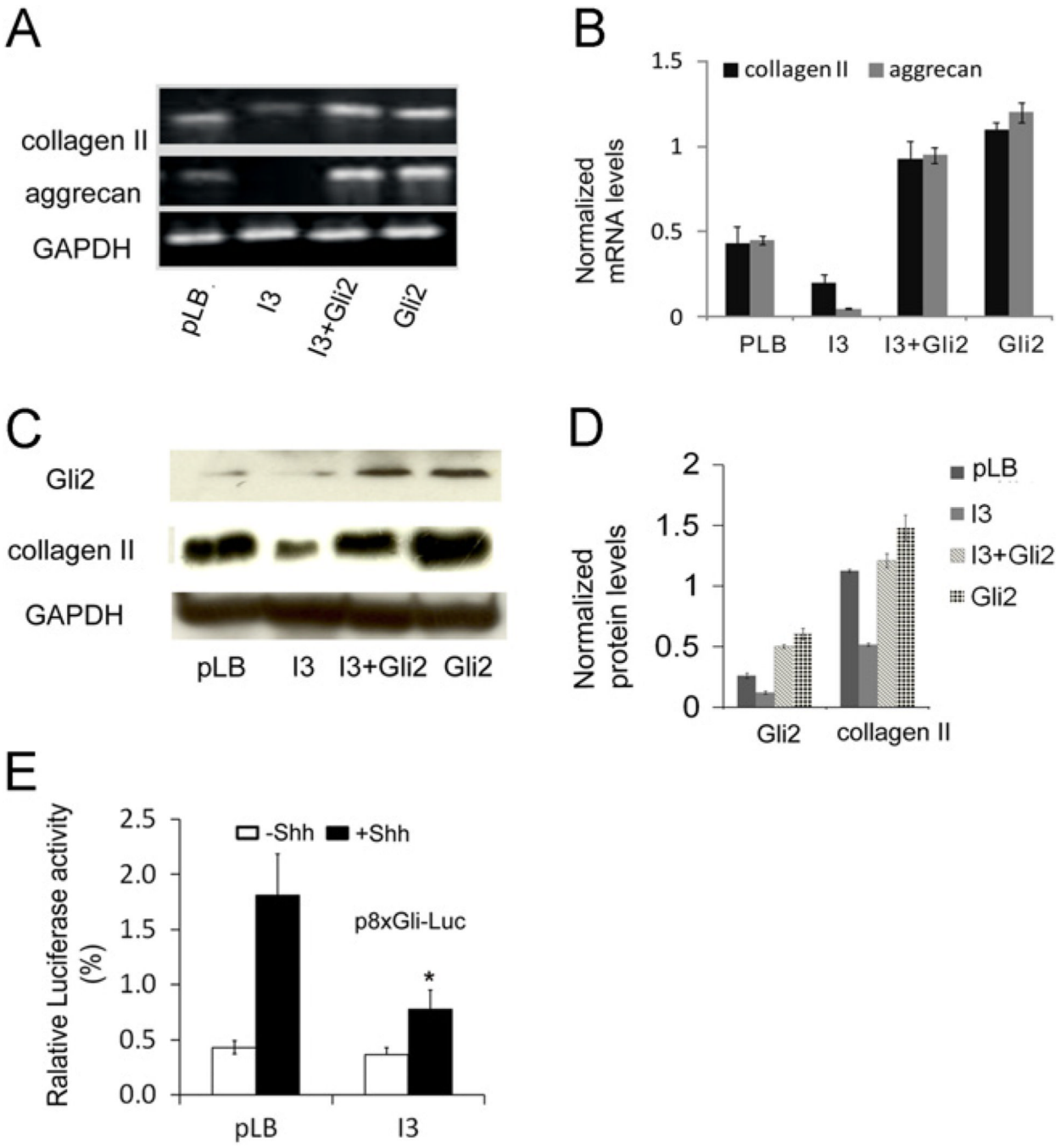

Fig. 4.

Silencing IFT80 dampens the Hh signaling pathway activity. (A) RT-PCR analysis of the chondrocyte differentiation markers collagen II and aggrecan. GAPDH served as a loading control. (B) Quantification of mRNA levels of the genes in A by normalization with GAPDH. Each band was quantitated by densitometry using ImageJ software. The bars represent the means ±SEM. *N* = 3. (C) Western blots for Gli2 and collagen II protein levels. GAPDH served as a loading control. (D) Quantification of the protein levels from the immunoblots shown in C. Each band was quantitated by densitometry using ImageJ software. The bars represent the means ±SEM. *N* = 3. (E) Hh luciferase reporter assay in

BMSC cells with or without 1 μg/mL sonic Hedgehog. The bars represent the means ±SEM. $N = 6$. *$P < 0.01$.

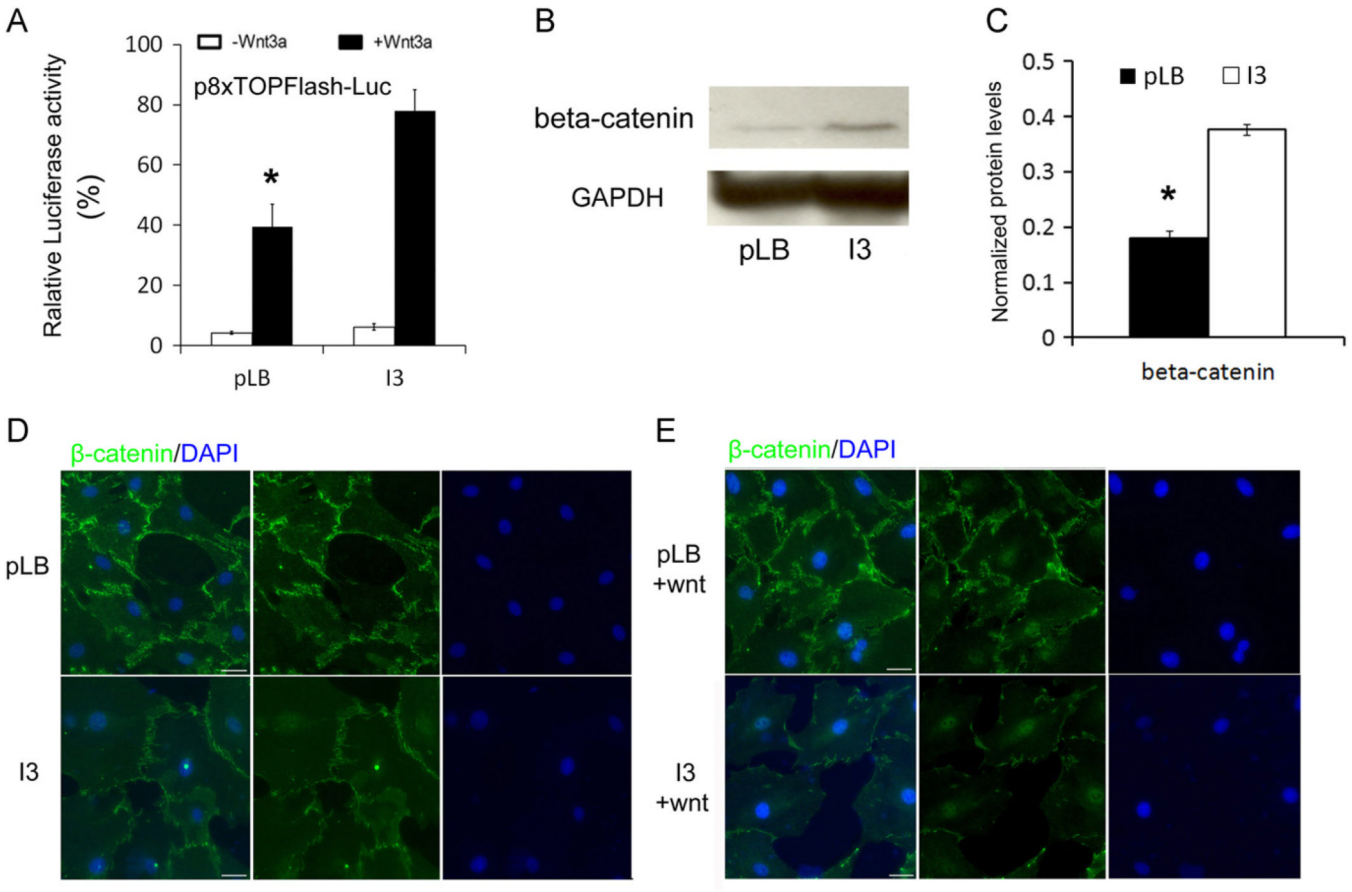

Fig. 5.

Silencing IFT80 enhances Wnt signaling activity. (A) Wnt luciferase reporter assay in BMSC cells with or without 100 ng/mL Wnt3a. The bars represent the means ±SEM. $N = 6$. *$P < 0.01$ pLB vs. I3, with Wnt3a treatment. (B) Relative expression levels of β-catenin in BMSCs infected with pLB and I3 were measured by Western blot. GAPDH was used as a loading control. (C) Quantification of the protein levels from the immunoblots shown in B. Each band was quantitated by densitometry using Image J software. The bars represent the means ±SEM. $N = 3$. *$P < 0.05$. (D) Immunostaining of mouse BMSCs infected with pLB or I3 for 48 h using β-catenin (β-catenin, green). The nuclei were labeled with DAPI (DAPI, blue). The cells were imaged on a Zeiss Axioimager microscope (20×). (E) Immunostaining of mouse BMSCs infected with pLB or I3 for 48 h using β-catenin (β-catenin, green). The cells were treated with 100 ng/mL Wnt3a for the last 24 h before staining. The nuclei were labeled with DAPI (DAPI, blue). The cells were imaged on a Zeiss Axioimager microscope (20×). The scale bar indicated 20 μm.